frontiers | Frontiers in Earth Science

TYPE Original Research
PUBLISHED 23 February 2023
DOI 10.3389/feart.2023.1095002



OPEN ACCESS

EDITED BY
Shuping Chen,
China University of Petroleum, China

REVIEWED BY
Jingshou Liu,
China University of Geosciences Wuhan, China
Li Wei,
China University of Petroleum, China

*CORRESPONDENCE
Lunyan Wei,
weilunyan@pku.edu.cn

SPECIALTY SECTION
This article was submitted to Structural Geology and Tectonics, a section of the journal Frontiers in Earth Science

RECEIVED 10 November 2022
ACCEPTED 08 February 2023
PUBLISHED 23 February 2023

CITATION
Wei L, Huang S, Luo C, Duan Y, Xia J, Zhong Z, Li X and Chang H (2023), Reconstruction of the proto-type basin and tectono-paleographical evolution of Tarim in the Cenozoic.
*Front. Earth Sci.* 11:1095002.
doi: 10.3389/feart.2023.1095002



# Reconstruction of the proto-type basin and tectono-paleographical evolution of Tarim in the Cenozoic

Lunyan Wei[1]*, Shaoying Huang[2], Caiming Luo[2], Yunjiang Duan[2], Jinkai Xia[1], Ziqi Zhong[1], Xiang Li[1] and Haining Chang[1]

[1]The Key Laboratory of Orogenic Belts and Crustal Evolution, Ministry of Education, School of Earth and Space Sciences, Peking University, Beijing, China, [2]Institute of Petroleum Exploration and Development, Tarim Oilfield Company, Korla, China

The Tarim Basin is the largest sedimentary basin in China, and it has experienced a complex tectonic evolutionary history. Reconstruction of the proto-type basin and tectono-paleogeography is helpful to understand the different stages of evolution of the sedimentary basin and basin-mountain relationship. It is significant to combine the basin with the regional tectonic background to discuss the process of basin-mountain coupling and the tectonic evolution of the peripheral orogenic belts. With a reliable residual thickness map and lithofacies map of the Tarim Basin in the Cenozoic, based on the amount of shortening we quantified from previous works and 81 balanced cross-sections, we restored the original range and compiled the proto-type basin map of Tarim Basin. From a compilation of previous studies on the lithofacies of peripheral blocks, the tectono-paleogeography of the Tarim Basin in Cenozoic has been reconstructed. The Indian Plate collided with the Eurasian continent at ~45–40 Ma. The remote effect of the collision led to the resurrection and reactivation of the Kunlun and Tianshan Mountains. The Southwest Tarim and Kuqa rejuvenated foreland basins separately developed along the north front of the Kunlun Mountains and the south front of the Tianshan Mountains. The tectonic evolution process of the Tarim Basin in the Cenozoic was divided into two stages: 1) in the Paleogene, the Neo-Tethys Ocean retreated stepwise westward from the Southwest of the Tarim Basin, and the sedimentary lithofacies of the Southwest Tarim Depression were bay lagoon facies and lake facies; 2) the Neo-Tethys Ocean retreat finally occurred in the Tarim Basin during the Late Oligocene to Early Miocene, and it became an almost closed terrestrial basin, with the deposition of fluvial facies and lacustrine facies. The Cenozoic tectono-paleogeography of the Tarim Basin is closely related to the closure of the Neo-Tethys Ocean and the reactivation of the Kunlun and Tianshan Mountains.

KEYWORDS

**Tarim Basin, Cenozoic, proto-type basin, tectono-paleogeographic evolution, basin-mountain**

## 1 Introduction

The Tarim Basin is the largest intracratonic basin in China and covers an area of 560,000 km$^2$. Source rocks for oil and gas were deposited widely in the Tarim Basin during different geological periods, including the Paleogene, and excellent oil and gas can usually be found in its marine rocks. The Tarim Basin is a natural laboratory with unique geological and geomorphological units, and can be divided into seventeen

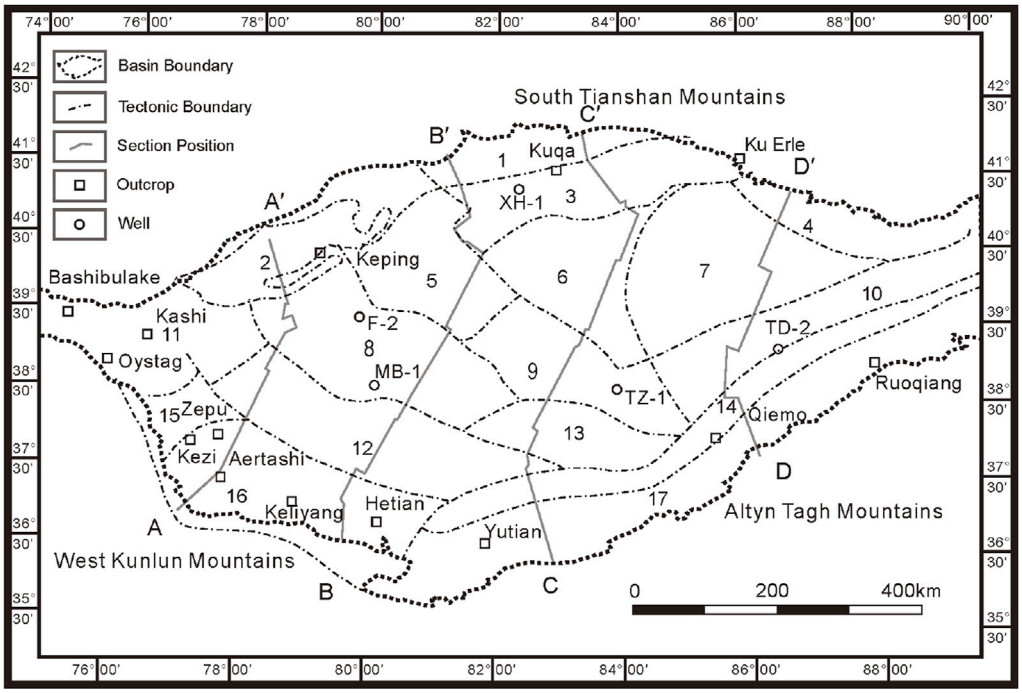


1-Kuqa Depression; 2-Kepingtage Faulted-uplift; 3-Tabei Uplift; 4-Kongquehe Slope; 5-Awati Depression; 6-Shuntuoguole Uplift; 7-Manjiaer Depression; 8-Bachu Uplift; 9-Tazhong Uplift; 10-Guchengxu Uplift; 11-Kashi Depression; 12-Maigaiti Slope; 13-Tangguzibas Depression; 14-Tanan Uplift; 15-Shache Bulge; 16-Yecheng Depression; 17-Southeast Depression

FIGURE 1
Schematic structural map of the Tarim Basin (modified after He et al., 2016; Laborde et al., 2019).

tectonic units in the Cenozoic (Dong et al., 2016; He et al., 2016) (Figure 1). Geographically bounded by the Western Kunlun Mountains, the Altyn Tagh mountain belt, and the Tianshan Mountains, the Tarim Basin has experienced a complicated tectonic history (Allen et al., 1993; Zhang et al., 2011; He et al., 2016; Laborde et al., 2019) (Figure 1).

In the early Cenozoic, the India-Asia collision caused large-scale intra-continental deformations (Liu et al., 2009; Fang et al., 2020). Under the far-field effect of the collision, a prominent tectonic salient formed on the Pamir plateau and the Pamir Salient experienced some northward translation (Lin et al., 2019; Li Y. P. et al., 2020). A major reactivation of the Western Kunlun Range occurred during the Cenozoic in response to the India-Asia collision (Tapponnier and Molnar, 1977; Laborde et al., 2019). A major reactivation of the Tian Shan also occurred during the Cenozoic in response to the India-Asia collision and this reactivation seems to have been initiated in the Oligocene with subsequent Miocene accelerations, which is supported by evidence including sediment provenance and growth strata (Izquierdo-Llavall et al., 2018; Li et al., 2019). The Altyn Tagh Range was also reactivated during the Cenozoic due to the India–Asia collision and this reactivation seems to have been initiated in the Eocene with subsequent Oligocene to Miocene accelerations (Cheng et al., 2015; Zhao et al., 2016). The maximum principal stress direction in different areas of the Tarim Basin is diverse. In the north of the Tarim Basin, the maximum principal stress direction is mainly N-S and NNW-SSE (Huang et al., 2013). In the southwest, the maximum principal stress direction is mainly NE-SW; and in the southeast, the maximum principal stress direction is mainly NW-SE (Wang et al., 2007).

A schematic structural map and seismic cross-sections was constructed to document the Cenozoic deformation through the Tarim area (Figures 1, 2). In the Cenozoic, the Tarim Basin was in a stage of strong compression, and the continuous collision around the Tarim Block accommodated a large amount of Cenozoic compressive deformation (Li et al., 2007; Laborde et al., 2019). Ancient orogens around the Tarim Basin were rejuvenated, and a thick (up to ~10 km) and continuous Cenozoic sedimentary series, mainly supplied by the erosion of the surrounding mountain ranges (Wei et al., 2000; Jia, 2009; He et al., 2013), formed the rejuvenated foreland basin in Kuqa and Southwest Tarim (Laborde et al., 2019) and the complex fault system in Bachu Uplift (Ning et al., 2021; Zhang et al., 2021) (Figure 2). In the case of the Western Kunlun and Southwestern Tian Shan compressive systems, these foothills mainly formed the Basin-Mountain system at the edge of the Tarim Basin (Figure 2). Wide (from ~50 to ~150 km) and long (100 s of km) uplifts, such as the Bachu uplift, are visible to the west of the basin (Figure 2).

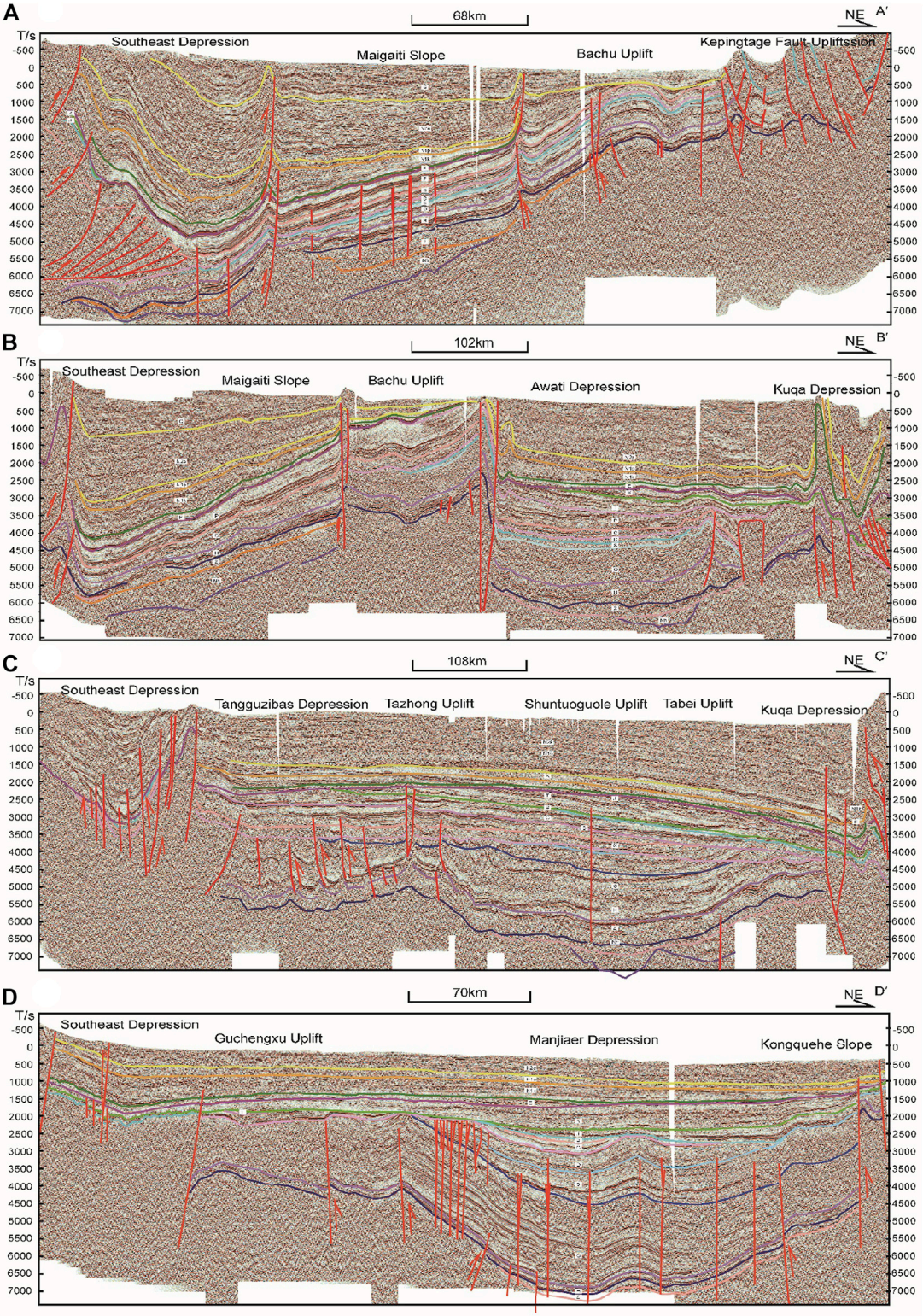


FIGURE 2
Four seismic cross-sections of the Tarim Basin (see Figure 1 for locations).

The far-field effect caused the reactivation of the Paleozoic and Mesozoic tectonic belts, changing the sea-land configuration in eastern Asia (Tapponnier et al., 1981; Wang et al., 2014; Lin et al., 2019; Li Y. P. et al., 2020). The Neo-Tethys Ocean retreated from Western Tarim in response to a combination of eustatic sea-level lowering, plate tectonics, and the autocyclic

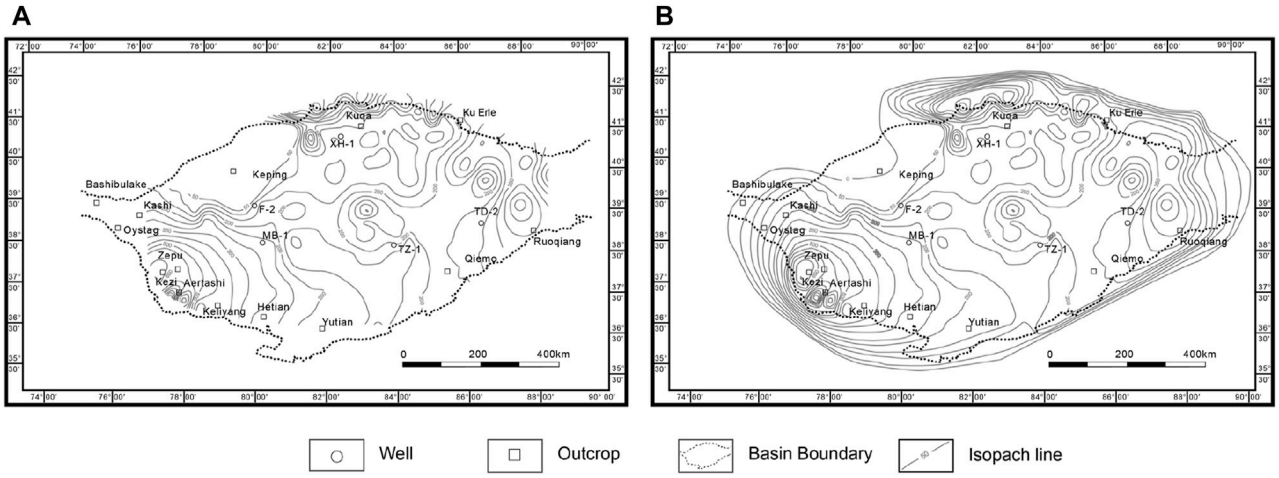


FIGURE 3
Schematic diagrams showing the steps of restoring the original thickness map, taking the late Paleogene restoration as an example. **(A)**: The residual thickness map of residual basin; **(B)** the pre-shortening original thickness map of the residual basin; thickness map contours show the depth (m) of the Upper Eocene to Oligocene in the Tarim Basin).

sedimentary infilling of the basin (Bosboom et al., 2011; Bosboom et al., 2014). At least five different seawater transgression-regression cycles occurred and the sea retreated from different parts of the Tarim Basin (Sun and Jiang, 2013; Bosboom et al., 2014; Sun et al., 2016a). The last regression marking the Tarim Basin generated a huge transformation from marine facies to terrestrial facies.

As a result of the collision of the Indian Plate and the Eurasian continent, the Tarim Block has different types of sedimentary facies from different stages of the Cenozoic. There are two issues to be addressed in this study: the tectono-paleogeographic evolution of the Tarim Basin and the tectonic interrelationships between the basin and the orogenic belts during the different stages. There are some studies that have mapped the lithofacies paleogeography of the Tarim Basin; however, several studies considered the whole basin and its periphery, and few compiled the proto-type basin by considering the India–Asia collision and the huge shortening of the basin. In this study, we restored the proto-type basin of the Tarim Basin and reconstructed the Tectono-paleogeographic evolution around the Tarim Basin in the Cenozoic, analyzing the changes of the paleo-geographical environment and Cenozoic deformation of the Tarim Basin and its periphery. When and how the retreat of the Neo-Tethys Ocean occurred were specially considered to reconstruct the proto-type basin and tectono-paleogeography of the Tarim Basin and its periphery.

## 2 Methodology and database

Guided by three steps of map compilation, we reconstructed the proto-type basin and tectono-paleogeography of the Tarim Basin and its periphery in the Cenozoic.

First, we restored the original thickness map (Figure 3). Based on the analysis of wells and outcrops in the whole basin, the lithofacies-paleographic maps in the range of the present basin were reliable. If there were border facies in the basin, they could be used to help delineate the scope of the basin. If there were none, to recover the denudation area, it was necessary to reconstruct the original thickness map based on the Cenozoic residual thickness map with thickness trend analysis (Figure 3). For an intracratonic basin, the thickness line needed to be concentric and closed. While for the foreland basin, the thickness line needed to be asymmetrical and the distance of each thickness line outside the basin at one-half of the inside. Therefore, the scope of the foreland basin was relatively narrow, and the terrane was near the Tarim Block.

Second, we restored the range of the proto-type basin, which meant restoring it to what it was before shortening or extension. The balanced cross-section method (Lou et al., 2016; Laborde et al., 2019) is one of the most practical ways to obtain the proto-type basin boundary. Based on previous balanced sections (Laborde et al., 2019), 71 balanced sections provided by Tarim Oilfield, and 10 balanced sections restored by us (Figure 4), we quantified the shortening and reconstructed the boundary of the pre-shortening proto-type basin.

Third, we restored the tectonic configuration of the Tarim Block and its adjacent plates during the development of the proto-type basin. After clarifying the sedimentation and deformation of the Tarim Basin, it was essential to clarify the peripheral margin of the Tarim Basin and the tectonic relationship between the Tarim Basin and its surrounding plates. To compile the proto-type basin maps and the tectono-paleogeographic maps, it was essential to figure out the answers to some questions: 1) the lithofacies distribution of the Tarim Basin in the Paleogene and Neogene (Guan and Guan, 2002; Shao et al., 2006; Yue et al., 2017; Ma CM. et al., 2020); 2) the paleogeographic distribution in its adjacent plates (Wang, et al., 2019; Ma T. et al., 2020; Song et al., 2022); 3) the sea retreat process of Neo-Tethys and its effect on the Tarim Basin (Bosboom et al., 2011; Bosboom, 2013; Sun and Jiang, 2013; Bosboom et al., 2014; Sun et al., 2016b; Li Q. et al., 2020; Sun et al., 2021).

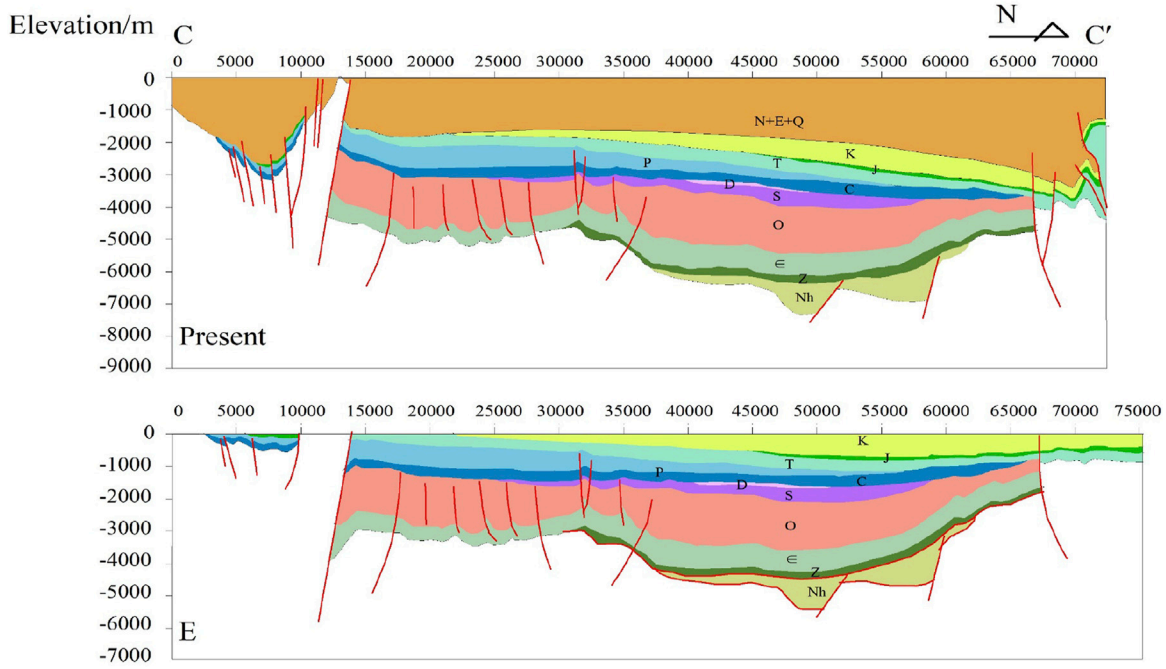


FIGURE 4
Balanced cross-section of CC′ (see Figure 1 for location).

**TABLE 1** Cenozoic stratum in the Tarim Basin (Ding et al., 1993; 2011; Guo, 1994; Jia et al., 2004; Shao et al., 2006; Li et al., 2017).

| Strata | | Southwest Tarim | | North Tarim | | Southeast Tarim |
|---|---|---|---|---|---|---|
| Quaternary | Lower Pleistocene | Xiyu | | Xiyu | | Xiyu |
| Neogene | Pliocene | Atushi | | Kuche | | Kuche |
| | Miocene | Wuqia | Pakabulake | Kangcun | | Kangcun |
| | | | Anjuan | Jidike | | Jidike |
| | | | Keziluoyi | Suweiyi | | Suweiyi |
| Paleogene | Oligocene | Kashi | Bashibulake | Kulugeliemu | Awate | Kulugeliemu |
| | Eocene | | Zhuoyoulegansu | | Xiaokuzibai | |
| | | | Wulagen | | | |
| | | | Kalatar | | | |
| | | | Gaijitage | | | |
| | Paleocene | | Qimugen | | | |
| | | | Aertashi | | | |
| | | Tuyiluoke | | | Talak | |

Based on previously published data (Laborde et al., 2019) and our new data, we obtained the proto-type basin maps and the tectono-paleogeographic maps in the Cenozoic. It is noteworthy that the biggest difference between the proto-type basin map and the tectono-paleogeographic map is the latter includes larger geographical range, which provides more information with the tectonic configuration of the Tarim Basin and its adjacent plates.

## 3 Analysis

Before compiling proto-type basin maps, we clarified three issues: firstly, the division of the evolution stages in the Cenozoic; secondly, the marine sedimentation problem of the Tarim Basin in the Cenozoic; and thirdly, the quantified shortening amount of the Tarim Basin.

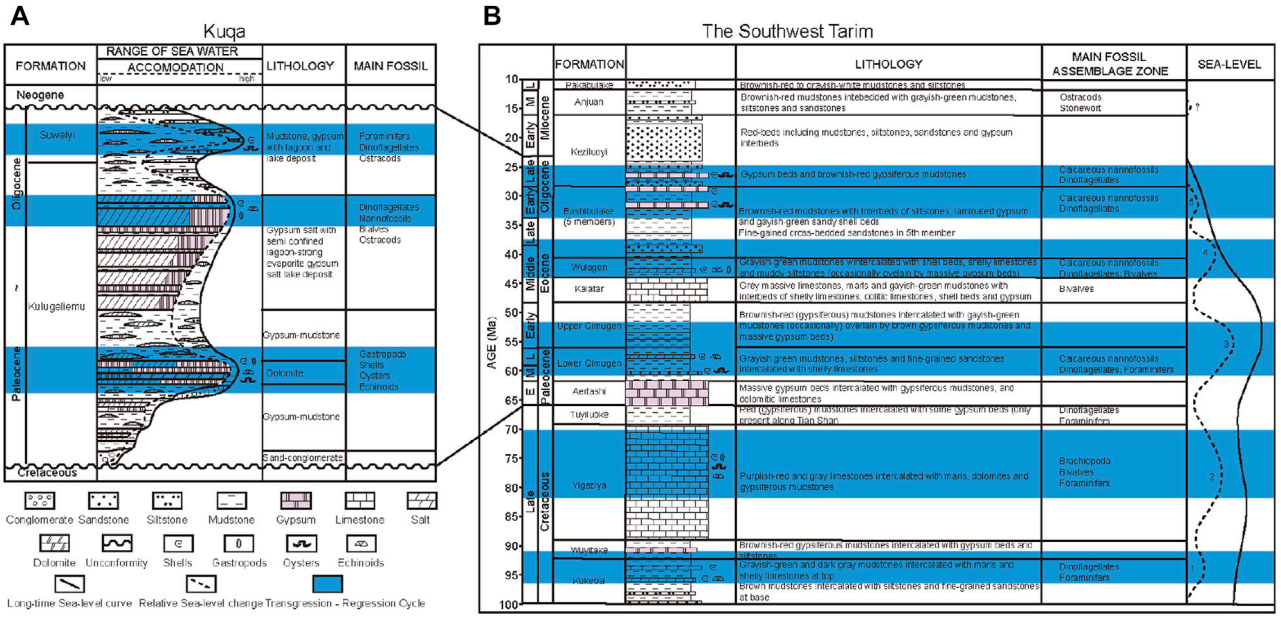


FIGURE 5
Simplified regional lithostratigraphic framework in Kuqa **(A)** and lithostratigraphic framework and main fossil assemblage zone of marine incursions in Southwest Tarim **(B)** (modified after Bosboom et al., 2011; Bosboom et al., 2014; Ma CM. et al., 2020).

## 3.1 Division of the evolution stages in the Cenozoic

The strata of the Cenozoic Tarim Basin were mainly exposed around the basin, and most of the basin was covered by desert. According to the sedimentary characteristics of Cenozoic strata in the basin, the Tarim Basin could be divided into three regions: Southwest Tarim, North Tarim, and Southeast Tarim (Table 1). Although there were different division schemes for Cenozoic stratigraphic subdivision in this area, in this study, the evolution stages in the Cenozoic were based on the stratigraphic subdivision unified as follows (Table 1).

In Southwest Tarim, the Paleogene strata included the Bashibulake Formation, Zhuoyoulegansu Formation, Wulagen Formation, Kalatar Formation, Gaijitage Formation, Qimugen Formation, and Aertashi Formation in the Kashi Group; the Neogene strata included the Pakabulake Formation, Anjuan Formation, Keziluoyi Formation in the Wuqia Group and the Atushi Formation (Table 1). In North Tarim, the Paleogene strata included the Awate Formation, Xiaokuzibai Formation, and Talak Formation in the Kulugeliemu Group; the Neogene strata included the Kuche Formation, Kangcun Formation, Jidike Formation, and Suweiyi Formation (Table 1). In Southeast Tarim, the Paleogene strata included the Kulugeliemu Group; the Neogene strata included the Kuche Formation, Kangcun Formation, Jidike Formation, and Suweiyi Formation (Table 1).

Since the Paleogene, the tectonic compression caused the uplift of the surrounding mountains around the Tarim Basin, while the basin itself was relatively stable (Wang et al., 2014; Laborde et al., 2019; Li Y. P. et al., 2020). During the Neogene, with the uplift of the Qinghai - Tibet Plateau, there are long-term growth and erosion in the mountain ranges and caused progressive thrusting over the Tarim basin (Jolivet et al., 2010; Wang et al., 2014; Laborde et al., 2019). Since the Quaternary, the Tarim Basin was surrounded by high mountains, progressively soil drying and forming China's largest inland water system and the largest desert.

## 3.2 Marine sedimentation problem of the Tarim Basin in the Cenozoic

According to the long-term eustatic trend of the Tarim Basin, there were at least five episodes of marine incursion in the Tarim Basin from the Cretaceous to the Paleogene (Figure 5), which are supported by Cretaceous-Paleogene sedimentary records (Bosboom et al., 2011; Bosboom, 2013; Bosboom et al., 2014; Li et al., 2017; Zhang et al., 2018). There are reliable pieces of evidence to restrict the time of the fourth and fifth incursions and the sea retreat to the Cenozoic (Bosboom et al., 2011; Bosboom et al., 2014; Zhang et al., 2018) (Figure 5).

The palaeomagnetic chronology and paleoenvironmental records of Cenozoic sections indicate that the fourth sea retreat from Aertashi occurred at ~41 Ma (Bosboom et al., 2014). Research on marine–terrestrial sediments at Oytag in the Early Cenozoic also suggests that the sea retreat from the Tarim Basin may have been diachronous (Sun and Jiang, 2013). The sea retreat from Oytag occurred in the Early Eocene at ~47 Ma and from Keliyang at ~45 Ma (Sun and Jiang, 2013; Sun et al., 2016a); the ~45 Ma peak in detrital zircon U/Pb was considered as an indication of a new sedimentary source (Wang et al., 2021).

Pieces of evidence, including the palaeomagnetic chronology and paleoenvironmental records, also restricted the fifth sea retreat occurring from Kuqa, Kezi, and Bashibulake to ~37 Ma and ~33–25 Ma (Bosboom et al., 2014) (Figure 5). In the Pamir-Tianshan convergence zone, the successions changed from marine deposits in the lower, continental clay, fine sand in the middle, and molasse in the upper part, recording the climate changes and evolution of the sea retreat (Wang et al., 2014). Small-scale sea incursions still occurred when the Neo-Tethys Ocean retreat occupied the Tarim Basin, which is supported by the sulfur isotope of gypsums or anhydrites in Kuqa ($\delta^{34}S$ from 11.6‰ to 15.9‰ in the Middle Paleocene, from 12.7‰ to 15.9‰ in the Late Eocene) (Zhang et al., 2013). Particle size analysis of the Suweiyi Formation sediments of the Southwest Tarim Depression indicated the sand was similar to near-shore sedimentary environments including lagoons and shallow lake facies (Tang et al., 2014). The lakes in the Jidike Formation were generally broad and shallow, and the lake shoreline was in response to both climate change and tectonic activities (Ma CM. et al., 2020).

Marine and lagoon deposits with fossils were recognized from southwest to the north, which was more than a thousand of kilometers by the outcrop and wells of the Miocene formations of the northern Tarim Basin (Guo et al., 2002). There were thin gypsum interbeds of marine strata in the Late Oligogene Suweiyi Formation in the Kuqa and Late Oligogene Keziluoyi Formation reserved in Southwest Tarim (Guo et al., 2002; Ma T. et al., 2020) (Figure 5). These fossils, including Foraminifer, Dinoflagellates, Ostracods, and Calcareous nannofossils, would seem to suggest that the range of seawater influence in the Early Miocene included two main areas, Kuqa and Southwest Tarim (Figure 5B). The high saline concentration of saltwater deposits with Foraminifer and Ostracods identified in Kuqa and Southwest Tarim showed that two lagoon bays in the western Tarim Basin were linked to the residual sea in the Late Oligogene or even until the early Miocene (Guo et al., 2002). However, from the Late Miocene to the Pliocene, the marine or lagoon environments vanished completely, and lake and freshwater deposits with Stonewort were common in the Tarim Basin (Guo et al., 2002) (Figure 5B).

The final time of the retreat of the Neo-Tethys Ocean from the Tarim Basin remains controversial. Some believe it was in the Early Oligocene (Bosboom et al., 2011; Sun and Jiang, 2013; Sun et al., 2016b), while others believe it occurred in the Late Miocene (Guo et al., 2002). Re-evaluating the fossil evidence and sedimentary facies (Figure 5), it was concluded that the final sea retreat occurred at 37–25 Ma, and the lagoon environments in the southwest and northwest of the Tarim Basin linked to the Neo-Tethys Ocean during the Late Oligocene. Taken together, these studies supported the notion that, as suggested by the presence of marine fossils and gypsum deposits, stepwise and diachronous sea retreat from the southwestern and northwestern margins of the Tarim Basin occurred in the late Oligocene—early Miocene.

## 3.3 Shortening amount of the Tarim Basin

The tectonic configuration of the Tarim Basin and its adjacent plates played an important role in the reconstruction of the proto-type basin because the compressive component of Cenozoic deformation controlled the basin (Wei et al., 2000; Li et al., 2007; Li Y. P. et al., 2020), with up to ~66.7% of compressive deformation accommodated in the Cenozoic orogeny (Laborde et al., 2019). Previous studies have explored the quantified compressive component (Li et al., 2007; Laborde et al., 2019). A regional-scale balanced cross-section constructed on Southwest Tarim—Kuqa including foreland fold-thrust showed a 64% shortening rate for Southwest Tarim and 30.6% for Kuqa (Li et al., 2007). Detailed analysis and examination found that most of the Cenozoic compressive deformation (from ~94% to 100%) was concentrated in the mountains along the basin margins, which meant it was negligible (up to ~6%) within the Tarim Basin (Laborde et al., 2019). Therefore, it was of great importance to restore the original thickness isopaches and determine the pre-shortening tectonic configuration of the Tarim Basin.

We calculated the shortening amount of every cross-section and quantified them into four representative profiles: AA′, BB′, CC′, and DD′ (Table 2) (Figure 1). According to the quantified data, we enlarged the range of the pre-shortening original thickness map and considered the zero-thickness line as the boundary of the pre-shortening proto-type basin.

# 4 Reconstruction of the proto-type Tarim Basin

Due to the uplift of the mountains around the Tarim Basin in the context of the India-Asian collision, the Tarim Basin gradually became a closed continental sedimentary basin (Wang et al., 2014; Lin et al., 2019; Li Y. P. et al., 2020). The paleogeography of the Tarim Basin in the Cenozoic was also related to the evolution of the Neo-Tethys Ocean (Shao et al., 2006; Li et al., 2017; Zhang et al., 2018). The Paleogene strata in the Tarim Basin were bay lagoons and shore-shallow lake facies, and the Neogene strata were flood plain-salt lakes and fluvial-alluvial fan facies (Zhuang et al., 2002; Shao et al., 2006; Li et al., 2017; Yue et al., 2017; Wu et al., 2020). This study also mapped the proto-type basin in the Late Eocene to better understand the tectono-paleogeography evolution in the Cenozoic.

## 4.1 In the Late Eocene

The landform pattern of the Tarim Basin in the Paleocene was mainly characterized by uplift in the center with depressions in the north and south (Shao et al., 2006). A short-term invasion of seawater occurred in the Kuqa Depression and Southwest Tarim Depression from the Paleocene to the Late Eocene (Guo et al., 2002; Li et al., 2017; Zhang et al., 2018; Lin et al., 2019) (Figure 6), where there were marine sediments from tens to hundreds of meters thick deposited in fluvial-deltaic and shallow-water lacustrine settings (Shao et al., 2006).

The degree of seawater influence was decreasing in the Late Eocene due to the small-scale, stepwise Neo-Tethys Ocean retreat (Shao et al., 2006). When seawater came from the west, sabkha or the

**TABLE 2 Shortening estimates across the Tarim Basin and its periphery.**

| Mountains | | | Shortening (km) | | |
|---|---|---|---|---|---|
| | | | 1 | 2 | 3 |
| | | | Cenozoic (Laborde et al., 2019) | Paleogene | Neogene |
| N Tibet | W Kunlun | Transect A (A) | 32 | 20.64 | 10.55 |
| | | Transect B (B) | 35 | (20) | (10) |
| | Altyn Tagh | Transect C (C) | 0.9 | | |
| | | Transect D (D) | 0.3 | | |
| S Tianshan | SW Tianshan | Transect A (A′) | 36 | (12.6) | (11) |
| | | Transect B(B′) | 4 | 12.00 | 9.13 |
| | | Transect C (C′) | 22 | 13.33 | 12.51 |
| | SE Tianshan | Transect D (D′) | 0 | | |

Note: Shortening in brackets are speculated.

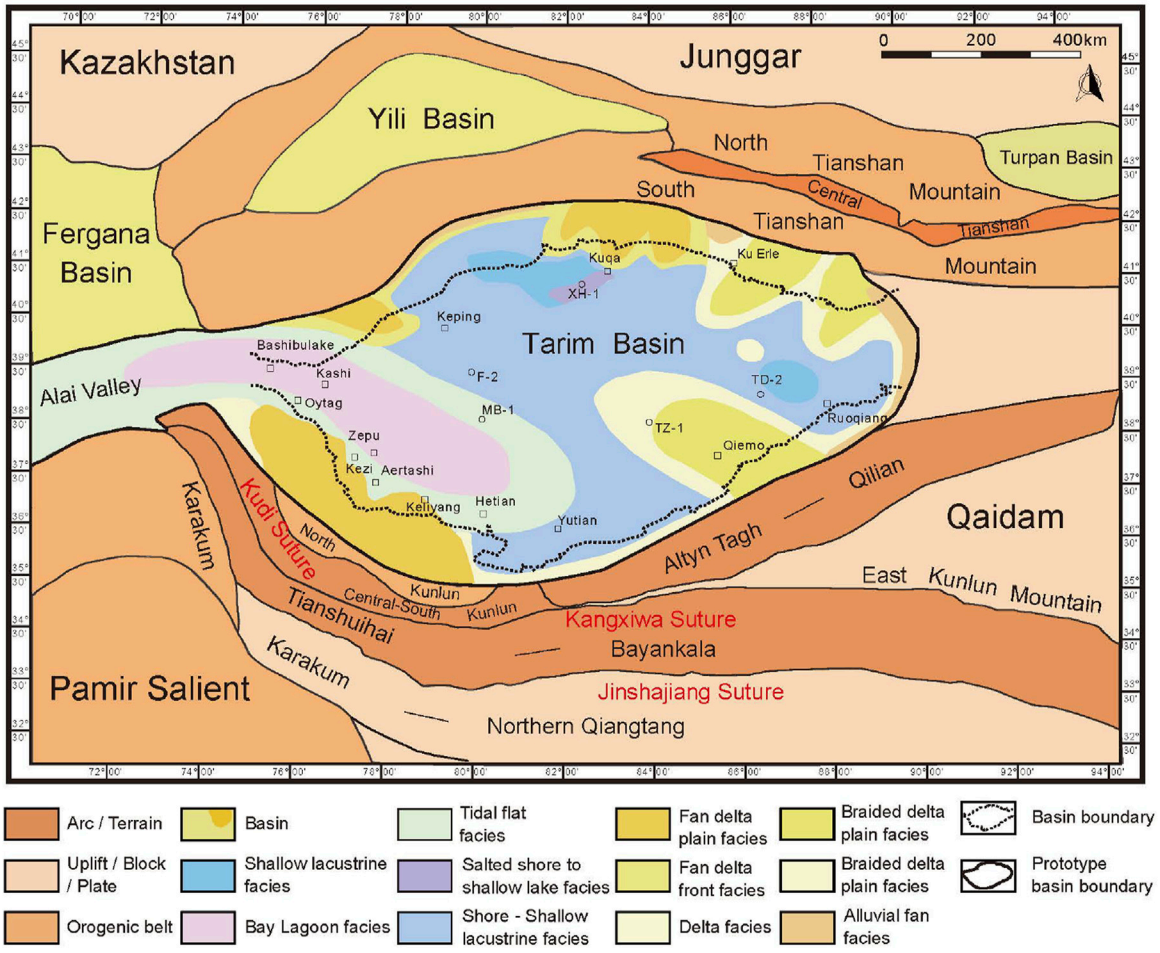


FIGURE 6
The Tarim proto-type basin and its periphery in the Late Eocene.

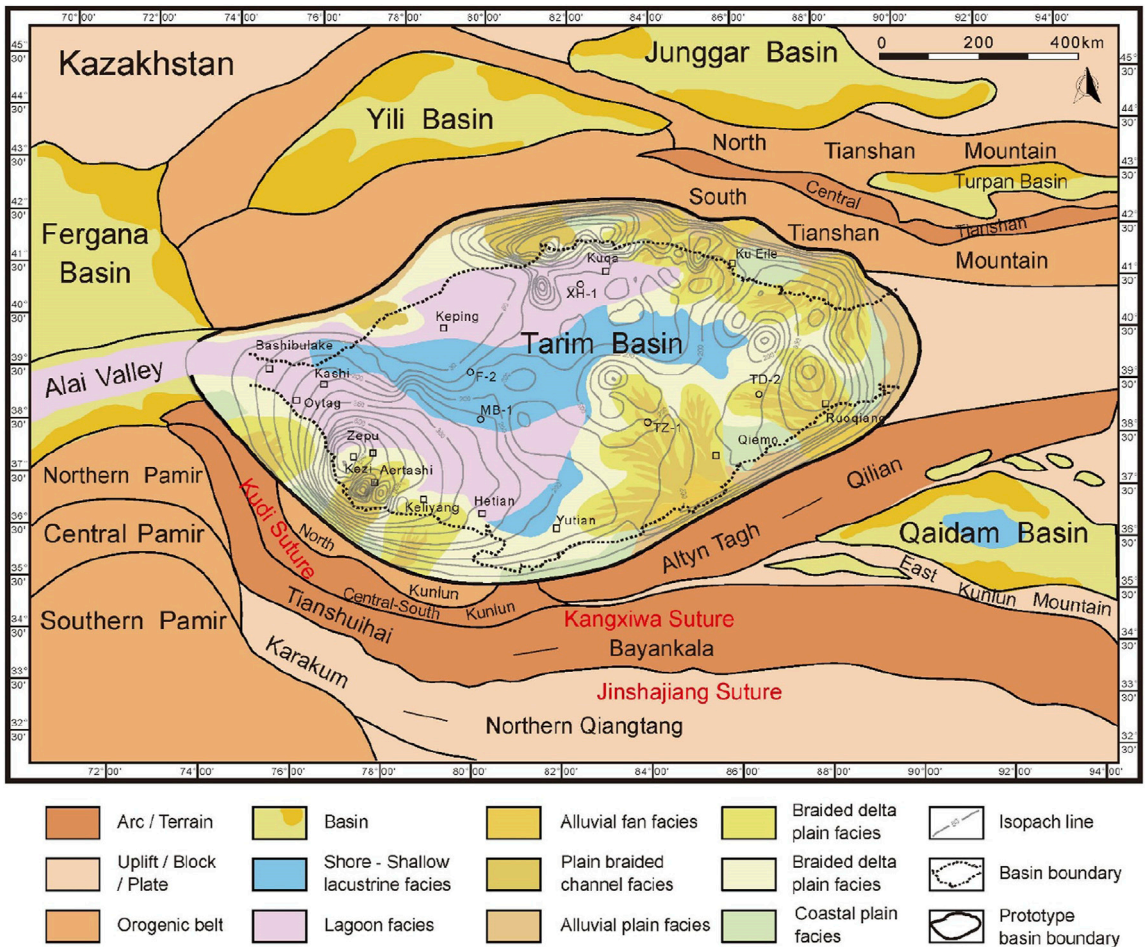


FIGURE 7
The Tarim proto-type basin and its periphery in the Late Oligocene. Thickness map contours show the depth (m) of the upper Eocene to Oligocene in the Tarim Basin.

open platform type of depositional environment was the most important sedimentary facies (Yue et al., 2017). Turning to the period of sea retreat, the basin fill was mainly composed of several typical facies, representing: bay lagoon facies and tidal facies dominated by carbonates and gypsum in the southwestern part; shore-shallow lacustrine facies dominated by sandstone, mudstone, carbonates, and gypsum in the northern part; and fluvial fan facies and fan delta facies dominated by conglomerate, sandstone, and siltstone along the basin margin (Shao et al., 2006; Li et al., 2013) (Figure 6).

The deformation and northward indentation of the Pamir Salient could have played an important role in controlling the lithofacies and sedimentary facies in the Tarim Basin. The provenance of the Cretaceous-Oligocene strata of the Southwest Tarim Depression was mainly from the Central Pamir (Sun et al., 2016a; Wang et al., 2021) (Figure 6), and the deposition center was near the West Kunlun Mountains (Shao et al., 2006). Regarding the Kuqa Depression, the provenance was mainly from the South Tianshan Mountains (He et al., 2004; Shao et al., 2006) (Figure 6), with the deposition center moving southward gradually (He et al., 2004).

## 4.2 In the Late Paleogene

The India-Asian collision had a remote effect on structural deformation and tectonic activity (Li et al., 2007; Jia, 2009; Laborde et al., 2019). For example, the West Kunlun reactivation was initiated in the Eocene with subsequent Oligocene to Miocene accelerations (Figures 2A, B), the Southwestern Tian Shan thrust wedge was formed above a decollement level (Figures 2A–C), and the Altyn Tagh strike-slip wedge was formed above a deep decollement level (Figures 2C, D).

In order to reconstruct the proto-type basin map of the Tarim Basin and its adjacent plates, we considered the structures activated during the Cenozoic and quantified the compressive component of this deformation. To the west, about 12.5 km of crustal shortening were accommodated in the Kuqa Depression, while to the east, about 20 km of crustal shortening were accommodated in the Southwest Tarim Depression (Table 2). Then we enlarged the range of the pre-shortening proto-type basin and combined the overall tectonic background. Separating the South Tianshan Mountains and the Pamir Salient was the intervening Alai Valley. The

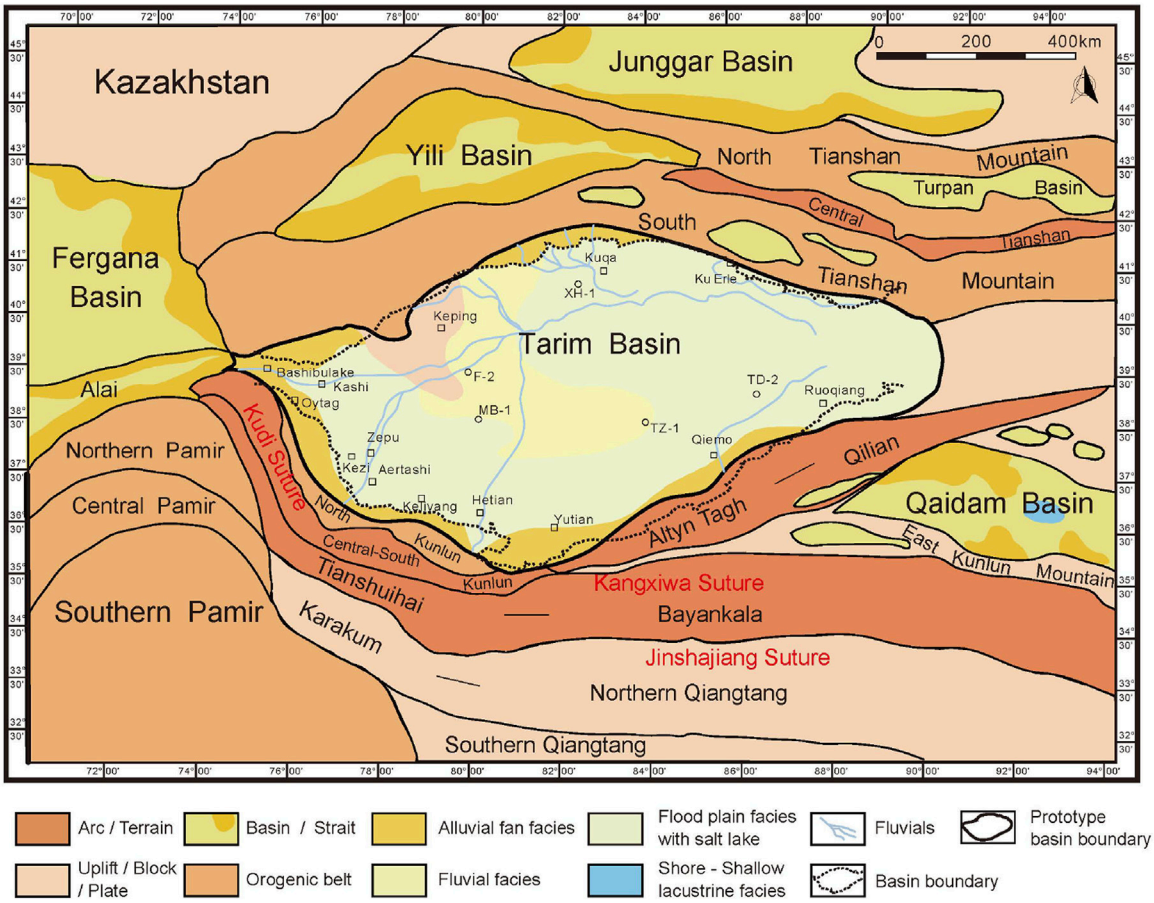


FIGURE 8
The Tarim proto-type basin and its periphery in the Late Neogene.

history of the Pamir Salient has been argued but data from new studies in the geology of Northern Pamir suggest that subsequent Cenozoic northward translation of the Pamir was interpreted to be only ~50 km and no more than ~80–100 km (Li Y. P.et al., 2020), establishing a greater degree of accuracy on the compressive component we quantified.

During the Late Eocene to Oligocene, the western part of the Tarim Basin contained an open marine, lagoon environment, with a continental environment in the eastern part (Zhang et al., 2022) (Figure 7). Eight sedimentary facies were divided in the study area, including lagoon facies, lacustrine facies, plain braided channel facies, braided delta facies, braided delta plain facies, alluvial plain facies, and alluvial fan facies, showing that the characteristics of spatial distribution in this area were from marine to continental (Figure 7). The Southwest Tarim Depression and Kuqa Depression could be identified as major deposition centers, where the maximum sediment deposition were both over eight-hundred-meters thick (He et al., 2004; Shao et al., 2006; Zhang et al., 2022). In Kuqa, the Suweiyi Formation was mainly composed of mudstones, siltstones, sandstones, and gypsum interbeds with nannofossils (Figure 5). In Southwest Tarim, mudstones with interbedded siltstones and laminated gypsum with nannofossils occurred in the Bashibulake Formation (Figure 5), which is evidence of the depositional environment of a lagoon.

However, whether the lagoon facies developed its range in the Late Oligocene is controversial. Based on the latest lithofacies-paleographic map of the Tarim Basin in the Suweiyi Formation provided by Tarim Oilfield, and combined with the analysis of the Neo-Tethys Ocean retreat (Figure 5), the outside seawater was linked to the western Tarim Basin *via* the Alai Valley, and the range of seawater influence in the Late Oligocene included two main areas, north to Kuqa and south to Southwest Tarim (Figure 7). In Kuqa, gypsum interbeds of marine strata and marine fossils developed in the Suweiyi Formation and Jidike Formation, which provides some support that lagoon facies developed in the Late Oligocene or even early Miocene. It could be concluded that the range of lagoon facies in the Late Oligocene was larger than the Late Eocene (Figures 6, 7). In the eastern part of the Tarim Basin, a continental sedimentary system existed from the basin margins to the center, from alluvial fan to braided river delta plain and braided river delta front (Shao et al., 2006; Zhang et al., 2022) (Figure 7).

### 4.3 In the Late Neogene

During the Neogene, the lasting tectonic compression caused the mountains surrounding the Tarim Basin to uplift and the basin closed, and the compressive component of the Neogene deformation could also be quantified. To the west, about 11 km of crustal shortening were accommodated in the Kuqa Depression, while to the east, about 10 km of crustal shortening were accommodated in the Southwest Tarim Depression (Table 2). Then we restored the range of the pre-shortening proto-type basin and combined the overall tectonic background. Compared with the Late Paleogene, the mountains, such as the Tianshan Mountains and West Kunlun Mountains, were reactivated by the ongoing structure deformation and tectonic activity (Figures 7, 8). A northward indentation of the Pamir Salient in the Cenozoic, causing a lower amount of shortening documented along the Alai Valley, and the basins, such as the Tarim Basin and the Qaidam Basin, were considered to have undergone continuous aridification.

Compared with the proto-type basin map of the Tarim Basin and its adjacent plates in the Late Eocene and Late Oligocene, the depositional environment of the Tarim Basin significantly changed in the Oligocene—Miocene: marine facies disappeared, and continental sedimentation patterns formed (Figures 6–8). The sea retreated from the whole Tarim Basin in the Late Neocene, and the Tarim Basin gradually graded to a closed inland environment (Figure 8). The Tarim Basin contained terrestrial depositional environments, such as alluvial fan groups, deltas, and flood plain facies with salt lakes (Figure 8). There were large thick molasse units near the deposition center in the Southwest Tarim Depression and Kuqa Depression, while toward the Bachu Uplift the thickness decreased gradually (Wu et al., 2020).

In the Neogene, it was still active on the south edge of the Tianshan mountain, the deformation was influencing the northern edge of the Tarim Basin (Jolivet et al., 2010). The deposition center of the Kuqa Depression gradually moved north to south and the thickness of the sediment increased (He et al., 2004). Several tectonic stages occurred in the Pamir-Tianshan convergence zone in the Cenozoic, and alluvial deposits dominated the sequences from the early Miocene (Wang et al., 2014) (Figure 8). The reactivation event of the Bachu Uplift could be linked to the India-Asian collision, where there were thrust fault systems may related to a deep decollement within the basement below the Tarim Block (Laborde et al., 2019) (Figures 2A, B).

Based on the lithofacies-paleographic map of the proto-type basin and our calculations of the quantified shortening (Table 2), and combined with the regional tectonic configuration, the Tarim proto-type basin and its periphery in the Late Eocene (Figure 6), Late Oligocene (Figure 7), and Late Neogene (Figure 8) was obtained. When comparing the proto-type basin and its periphery in the Late Eocene (Figure 6) and in Late Oligocene (Figure 7), the biggest difference that could be seen was that the range of seawater influence became larger and the range of lagoon facies increased from the Southwest Tarim Depression to the Kuqa Depression (Figure 7). This variation indicated that there was still an intermittent connection between the Tarim Basin and the Neo-Tethys Ocean that occurred separately during the third, fourth, and fifth transgression-regression events in the Paleogene (Figure 5), as well as the final sea retreat which occurred at 25–30 Ma in the Late Oligocene (Figure 5) or even the early Miocene.

## 5 Reconstruction of the tectono-paleogeography around the Tarim Basin

To obtain the tectono-paleogeographic map around the Tarim Basin in the Cenozoic, more studies were considered, such as the configuration of the plates around the Tarim Block in Asia, the lithofacies and paleogeography of basins in the adjacent plates, especially in the central Asian plates (Wang, et al., 2019; Zhang et al., 2019; Ma T. et al., 2020; Song et al., 2022), and the proto-type basin map of the Tarim Basin and its periphery in the Cenozoic we compiled (Figures 7, 8).

### 5.1 Continued subduction of the Indian ocean in the Late Paleogene

In the long-term paleo-geographical evolution in the Cenozoic, as the global sea levels fell, the Neo-Tethys Ocean retreat gradually occurred from the Junggar Basin and the Tarim Basin, and the Fergana Basin and the Alai Valley in southern Kyrgyzstan, and the Afghan–Tajik Basin (Bosboom et al., 2011; Carrapa et al., 2015; Li et al., 2017; Li Q. et al., 2020). In the Paleogene, the Neo-Tethys Ocean entered the western Tarim Basin *via* the present-day Alai Valley (Bosboom et al., 2011; Zhang et al., 2013; Bosboom et al., 2014) (Figure 9). The sea retreated westward in at least five transgressions in the west of the Tarim Basin during the Cretaceous-Cenozoic (Bosboom et al., 2011; Bosboom, 2013; Zhang et al., 2013; Bosboom et al., 2014), where tidal flat and lagoon facies associations were extended and carbonate reservoirs and mudstone covers were formed (Shao et al., 2006; Yue et al., 2017). The sedimentary lithofacies were reflected by the Neo-Tethys Ocean seawater, and developed lagoon facies in the Alai Valley and shore-shallow lacustrine facies in the east of the Tarim Basin (Guan and Guan, 2002; Guo et al., 2002; Ma CM. et al., 2020) (Figure 5).

For many decades, the time of the India-Asia continental collision has been debated. But it is accepted that the final collision was completed at ~45–40 Ma, followed by continued post-collisional convergence to the present (Xia et al., 2009; Bouilhol et al., 2013; Todrani et al., 2022). The Tibetan Plateau is still experiencing deformation (Liu et al., 2009), distributing a lot of Cenozoic basin groups (Song et al., 2022) (Figure 9). The northeastern margin of the Tibetan Plateau, which includes the North Qiangtang terrane and the South Qiangtang terrane as well as the Kunlun Mountains and the Qaidam Basin, continues to deform in response to the ongoing India-Asia collision (Liu et al., 2009; Fang et al., 2020). As a huge intermontane basin, the Qaidam Basin was dominated by lacustrine facies during the Oligocene (Wu et al., 2020) (Figure 9).

The tectonic evolution of the Pamir Salient in the Cenozoic has played an important role in controlling the shift from marine to continental sedimentation in the Tarim and Tajik Basins (Bosboom

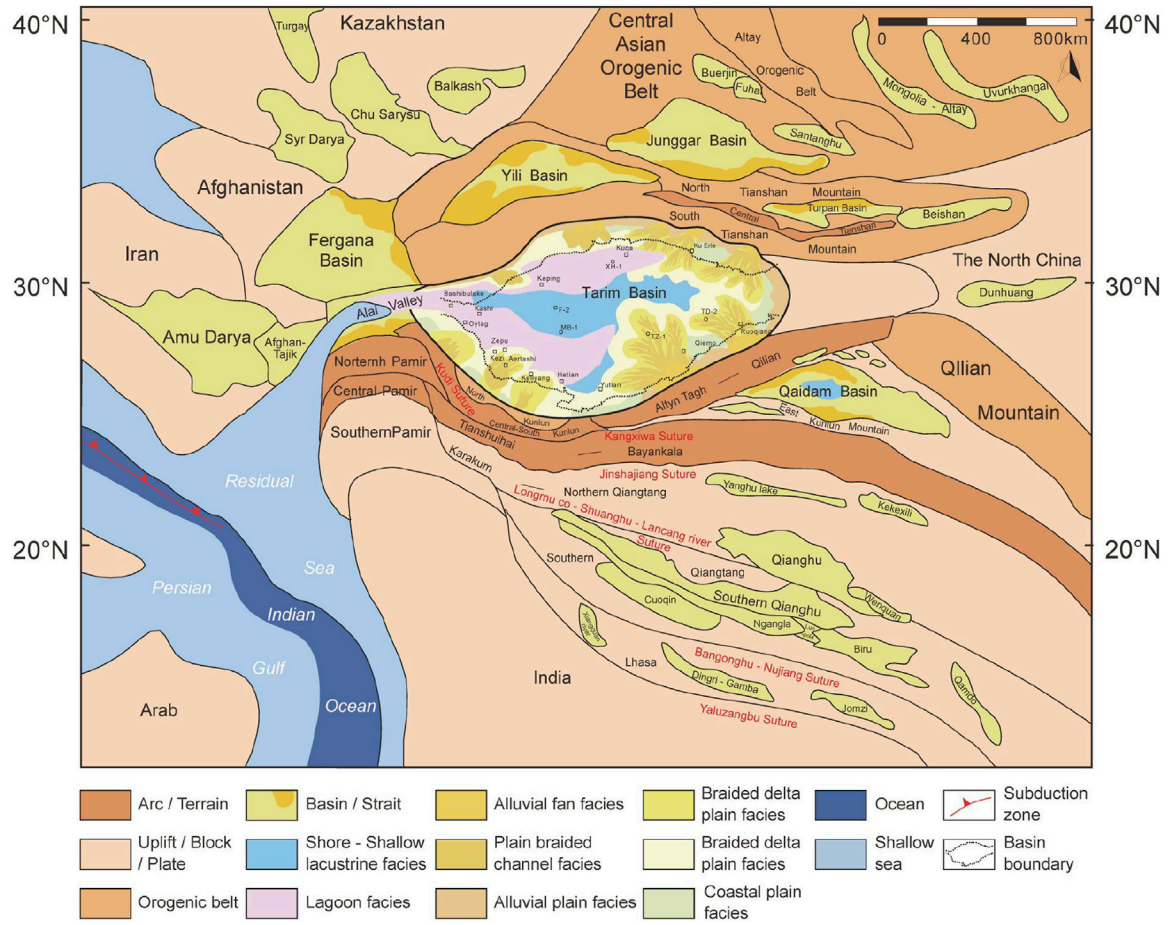


FIGURE 9
Tectono-paleogeography map around the Tarim Basin in the late paleogene.

et al., 2011; Sun and Jiang, 2013; Carrapa et al., 2015; Sun et al., 2016b). There were also basin groups distributed in Central Asia that experienced Paleozoic—Cenozoic sedimentary evolution including, for example, the Fergana Basin, Afghanistan-Tajik Basin, and Turgay Basin in the west, and the Junggar Basin and Santanghu Basin in the east (Figure 9) (Wang et al., 2019; Ma T. et al., 2020). Several intermontane basins, such as the Yili basin and the Turpan basin, were preserved within the interior of the TianShan Mountains (Figure 9) (Jolivet et al., 2010). In the west of the tectono-paleogeography map around the Tarim Basin in the Late Paleogene, a remnant Neo-Tethys Ocean branched *via* Alai Valley into a remnant marine embayment, causing the lagoon facies to develop in the Southwest Tarim Depression and Kuqa Depression in the northern Tarim Basin (Figure 9).

## 5.2 Basin-mountain system developed in the Late Neogene

The continental collision between the Arabian and Eurasian plates following the subduction of the Neo-Tethys Ocean beneath Eurasia resulted in a complex deformation across the Zagros Mountains (Figure 10). There was permanent closure of the northwestern segment of the Tethyan Seaway by 12.8 Ma in the Early-Middle Miocene (Homke et al., 2004; Pirouz et al., 2015; Sun et al., 2021). Both the complex mountain building deformation across the Zagros Mountains and the further northward indentation of the Pamir Salient resulted in the closure of the Alai Valley and a complete sea retreat from the Tarim Basin (Figure 10). The sea retreat was the one of the most significant events during the Late Oligocene—Early Miocene, causing the biggest differences in the southwest of the Tarim Basin (Figures 9, 10).

As the India-Asia continental collision is still ongoing, the Pamir Salient is still experiencing deformation. Intraplate orogeny occurred in the Kunlun Mountains and Tianshan Mountains due to the strong remote effect in the Miocene. In the mountains surrounding the Tarim Basin, mainly at the front of the Western Kunlun Mountains and Southwestern Tianshan Mountains, a significant fraction of the deformation was accommodated by new-formed structures during the Cenozoic (Li et al., 2007; Laborde et al., 2019). Accordingly, the margins of the Tarim Basin, mainly in the Southwest Tarim Depression and the Kuqa Depression, corresponded to the basin-mountain system and became rejuvenated foreland basins due to the intense regional

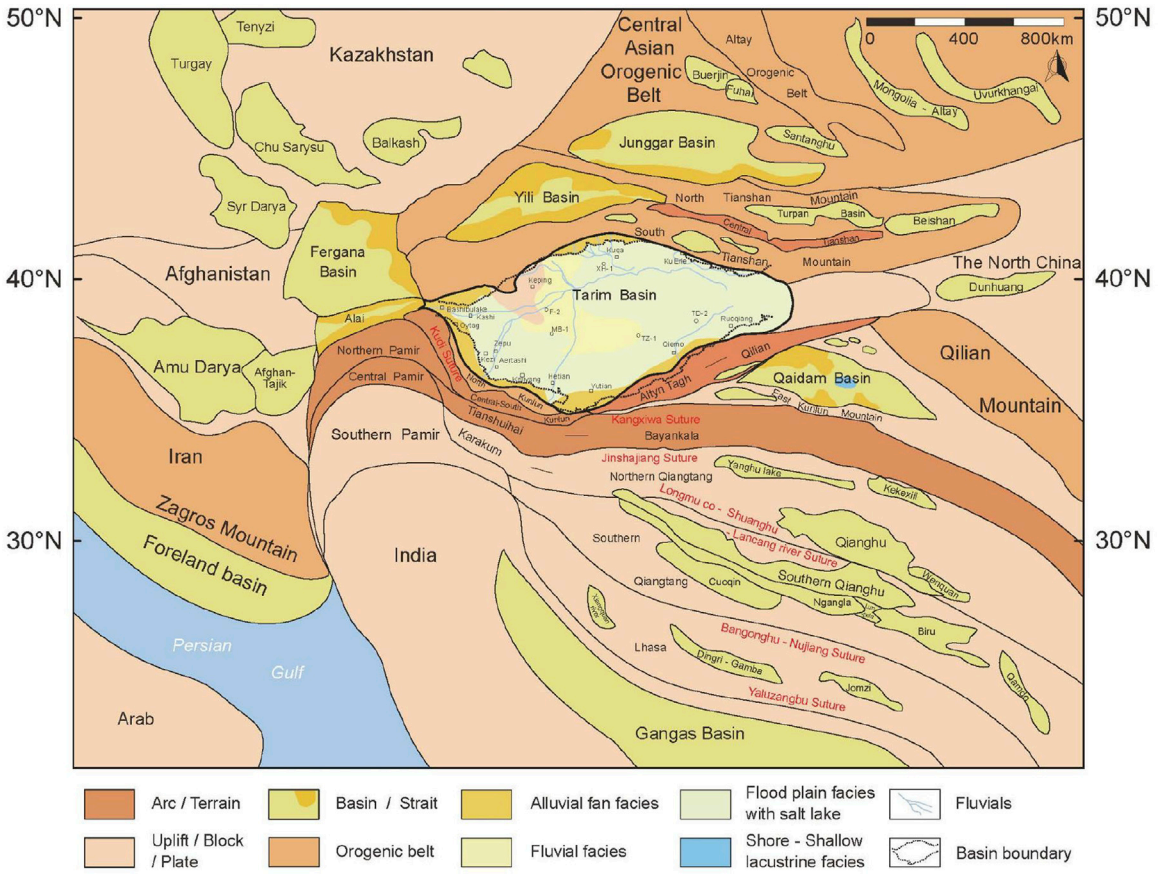


FIGURE 10
Tectono-paleogeography map around the Tarim Basin in the Late Neogene.

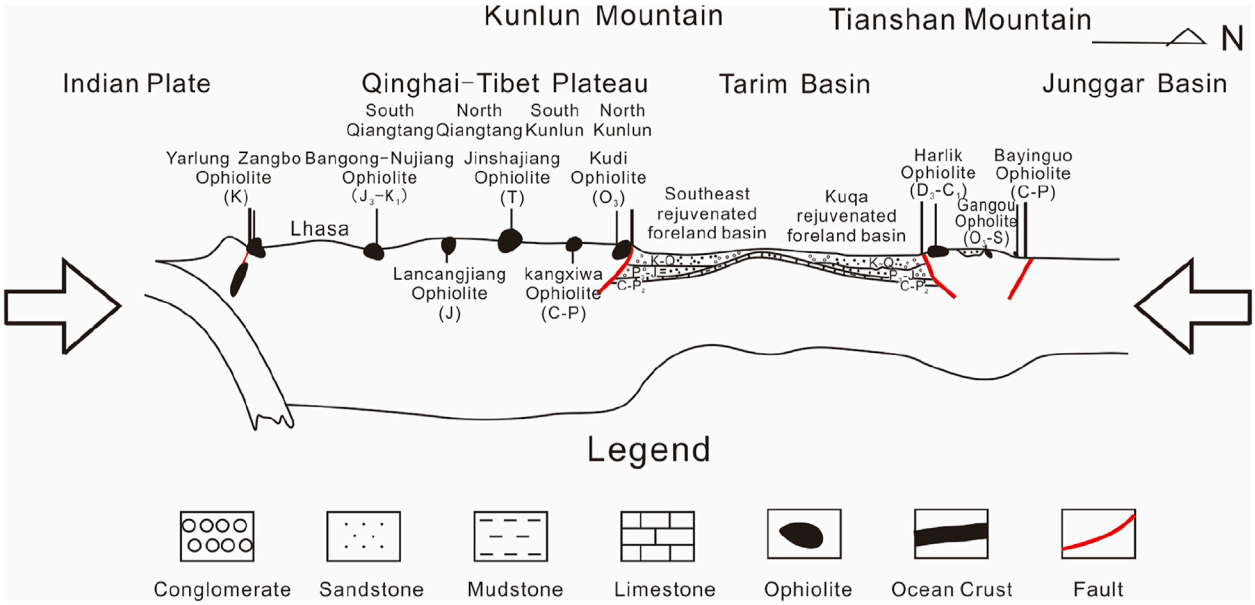


FIGURE 11
Tectonic evolution of the Tarim Basin from the Late Cretaceous to Cenozoic and its response to adjacent blocks and ocean evolution.

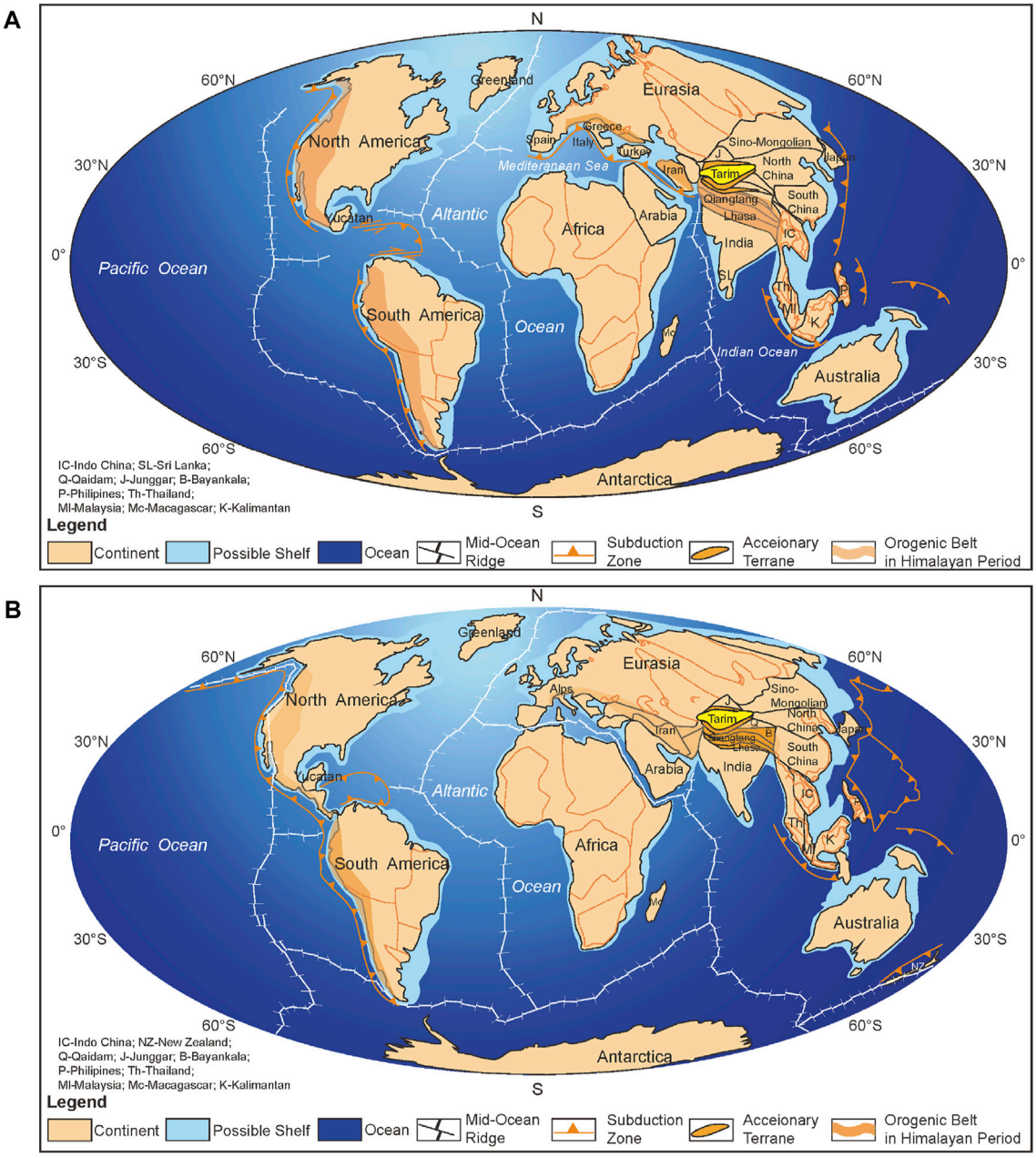


FIGURE 12
Global plate reconstruction in the late Paleogene **(A)** and Late Neogene **(B)** (modified after Scotese, 2004).

compression (Wei et al., 2000; Wang et al., 2020) (Figures 10, 11).

The present-day topography of the Tarim Basin and its surrounding mountains and adjacent blocks is considered to be related to the ongoing India-Asia collision (Figures 9–11). In the Cenozoic, the Western Kunlun Mountains and the South Tianshan Mountains were rejuvenated, and the Southwest Tarim Depression and Kuqa Depression formed rejuvenated foreland basins (Figure 11). Associated with these compressive structures, the Bachu Uplift also corresponded to the rejuvenated Western Kunlun Mountains, forming steep bounding thrusts, in particular deep fault systems (Zheng et al., 2014; Laborde et al., 2019) (Figures 2A, B).

## 6 The Tarim Block in global plate tectonics and its evolution history in the Cenozoic

The Tarim Block occupies an important position in Central Asia and the tectonic configuration around the Tarim Block has been evolving in the Cenozoic. Based on studies by previously published papers about the Tarim Block in global plate tectonics and the regional geological background in the Cenozoic (Scotese, 2004; Ma CM. et al., 2020; Wang, et al., 2020; Song et al., 2022), we combined our newly compiled proto-type basin maps (Figures 6–8) and tectono-paleogeography maps (Figures 9, 10) to modify the

global plate reconstruction in the Late Paleogene (Figure 12A) and Late Neogene (Figure 12B). In our study, the Tarim Block was considered important and its response to adjacent blocks and ocean evolution were highlighted.

To the south of the Tarim Block, some terranes and blocks continue to deform, including the Tianshuihai, North Qiangtang, South Qiangtang, and Lhasa blocks, in response to the ongoing India-Asia collision (Figure 12). Since the collisions of the Lhasa Block and the India Plate with the Asian Plate in the Late Cretaceous, the mountains surrounding the Tarim Basin have rapidly uplifted, with a large amount of compressive deformation at the basin edges (Li et al., 2007; Jia, 2009; Laborde et al., 2019). To the north of the Tarim Block, the North and the South Tianshan Mountains were reactivated, and fold-and-thrust belts localized the topographic front of the mountain range (Jolivet et al., 2010; Jolivet et al., 2013; Laborde et al., 2019). The basins that formed on the Central Asian Orogenic Belt were small-sized continental basin groups (Song et al., 2022). To the Northwest of the Tarim Block, there were also some basin groups formed on the Kazakhstan Block, including the Syr Darya, Turgay, Chu-Sarysu, and Balkhash Basin (Wang et al., 2019; Ma T. et al., 2020).

Besides the long-lasting plate collision, global climate change was another key on the paleogeography and tectonic evolution of the Tarim Block and its adjacent blocks. As the global sea levels fell, the Neo-Tethys Ocean gradually retreated from Asian Plate in the Cenozoic (Sun and Jiang, 2013; Carrapa et al., 2015; Sun et al., 2016a; Li et al., 2020; Sun et al., 2021). The Tarim Basin has a paleogeographical evolution characterized by a long-term stepwise Neo-Tethys sea retreat punctuated by short-term shallow-marine incursions (Bosboom et al., 2011; Bosboom, 2013; Bosboom et al., 2014). The last incursion extended to the southwest and the north of the Tarim Basin with its marine deposits and fossil assemblages, and the sea retreated at ~37–25 Ma (Figure 12).

## 7 Conclusion

1. Several localized tectonic activities around the Tarim Basin occurred due to the ongoing India-Asia collision in the Cenozoic, causing tectono-paleogeography changes in the basin.
2. As the Neo-Tethys Ocean retreat finally occurred in the Tarim Basin during the Late Oligocene - Early Miocene, the proto-type basin of the Tarim Basin evolved from lagoon facies in the west and terrestrial facies in the east in the Paleogene to the evolution of terrestrial depositional environments in the Neogene.
3. By quantifying the compressive component of the Cenozoic deformation, it could be seen that the main part of the deformation was accommodated by the reactivated basin-mountain system, mainly in the edges of the Tarim Basin and surrounding ranges.

## Data availability statement

The original contributions presented in the study are included in the article/supplementary material, further inquiries can be directed to the corresponding author.

## Author contributions

LW did the main work and wrote the paper; SH, CL and YD provided the data; JX, ZZ, XL, and HC contributed to the map-compiling. All authors read and approved the final manuscript.

## Conflict of interest

SH, CL, and YD were employed by Tarim Oilfield Company.

The remaining authors declare that the research was conducted in the absence of any commercial or financial relationships that could be construed as a potential conflict of interest.

## Publisher's note



## References

Allen, M. B., Windley, B. F., and Zhang, C. (1993). Palaeozoic collisional tectonics and magmatism of the Chinese Tien Shan, central Asia. *Tectonophysics* 220 (1-4), 89–115. doi:10.1016/0040-1951(93)90225-9

Bosboom, R. E., Dupont-Nivet, G., Grothe, A., Brinkhuis, H., Villa, G., Mandic, O., et al. (2014). Timing, cause and impact of the late Eocene stepwise sea retreat from the Tarim Basin (west China). *Palaeogeogr. Palaeoclimatol. Palaeoecol.* 403 (2), 101–118. doi:10.1016/j.palaeo.2014.03.035

Bosboom, R. E., Dupont-Nivet, G., Houben, A., Brinkhuis, H., Villa, G., Mandic, O., et al. (2011). Late Eocene sea retreat from the Tarim Basin (west China) and concomitant Asian paleoenvironmental change. *Palaeogeogr. Palaeoclimatol. Palaeoecol.* 299 (3-4), 385–398. doi:10.1016/j.palaeo.2010.11.019

Bosboom, R. E. (2013). *Paleogeography of the central asian proto-paratethys sea in the Eocene [D]* (Utrech: Ph.D. thesis).

Bouilhol, P., Jagoutz, O., Hanchar, J. M., and Dudas, F. O. (2013). Dating the India–Eurasia collision through arc magmatic records. *Earth Planet. Sci. Lett.* 366, 163–175. doi:10.1016/j.epsl.2013.01.023

Carrapa, B., Decelles, P. G., Wang, X., Clementz, M. T., Mancin, N., Stoica, M., et al. (2015). Tectono-climatic implications of Eocene Paratethys regression in the Tajik basin of central Asia. *Earth Planet. Sci. Lett.* 424, 168–178. doi:10.1016/j.epsl.2015.05.034

Cheng, F., Guo, Z. J., Jenkins, H. S., Fu, S. T., and Cheng, X. (2015). Initial rupture and displacement on the Altyn Tagh fault, northern Tibetan plateau: Constraints based on residual mesozoic to cenozoic strata in the Western Qaidam Basin. *Geosphere* 11, 921–942. doi:10.1130/GES01070.1

Ding, X. Z., Lin, C. S., Liu, J. Y., Han, K. Y., Pang, J. F., and Pang, W. H. (2011). The sequence stratigraphic response to the basin-orogene coupling process of Cretaceous-Neogene in Tarim Basin, China. *Earth Sci. Front.* 18 (4), 144–157. (in Chinese with English abstract).

Ding, X. Z., Liu, X., Wu, S. Z., Fu, D. R., Yao, J. X., Wu, S. Z., et al. (1993). Discussion on the Cretaceous-Paleogenese dimentaty features and environments of Kuzigongsu area, Western Tarim basin. *Xinjiang Geol.* 11 (3), 179–193. (in Chinese with English abstract).

Dong, S. L., Li, Z., and Jiang, L. (2016). The early Paleozoic sedimentary–tectonic evolution of the circum-Mangar areas, Tarim block, NW China: Constraints from integrated detrital records. *Tectonophysics* 682, 17–34. doi:10.1016/j.tecto.2016.05.047

Fang, X. M., Dupont-Nivet, G., Wang, C. S., Song, C. H., Meng, Q. Q., Zhang, W. L., et al. (2020). Revised chronology of central tibet uplift (lunpola basin). *Sci. Adv.* 6 (50), eaba7298. doi:10.1126/sciadv.aba7298

Guan, S. Z., and Guan, S. Q. (2002). Stratigraphic age and depositional environment of Jidike Formation in Kuche basin of xinjiang [J]. *Geol. Chemial Minerals* (01), 1–6+22. (in Chinese with English abstract). doi:10.3969/j.issn.1006-5296.2002.01.001

Guo, X. P., Ding, X. Z., He, X. X., Li, H. M., Su, X., and Peng, Y. (2002). New progress in the study of marine transgressional events and marine strata of the meso-cenozoic in the Tarim Basin. *Acta Geol. Sin.* (03), 299–307. (in Chinese with English abstract). doi:10.3321/j.issn:0001-5717.2002.03.002

Guo, X. P. (1994). The stratigraphic division of the marine Paleocene in the Western Tarim basin [J]. *Geol. Rewiew* 40 (4), 322–329. (in Chinese with English abstract). doi:10.3321/j.issn:0371-5736.1994.04.005

He, B. Z., Jiao, C. L., Xu, Z. Q., Cai, Z. H., Zhang, J. X., Liu, S. L., et al. (2016). The paleotectonic and paleogeography reconstructions of the Tarim Basin and its adjacent areas (NW China) during the late Early and Middle Paleozoic. *Gondwana Res.* 30, 191–206. doi:10.1016/j.gr.2015.09.011

He, D. F., Li, D. S., He, J. Y., and Wu, X. Z. (2013). Comparison in petroleum geology between Kuqa depression and Southwest depression significance. *Acta Geosci. Sin.* 34 (02), 201–218. (in Chinese with English abstract). doi:10.7623/syxb201302001

He, G. Y., Lu, H. F., Yang, S. F., and Li, S. X. (2004). Subsiding features of the mesozoic and cenozoic Kuqa basin, northwestern China. *J. Zhejiang Univ.* (01), 110–113+120. (in Chinese with English abstract). doi:10.3321/j.issn:1008-9497.2004.01.024

Homke, S., Verges, J., Garces, M., Emami, H., and Karpuz, R. (2004). Magnetostratigraphy of miocene–pliocene Zagros foreland deposits in the front of the push-e kush arc (lurestan province, Iran). *Earth Planet. Sci. Lett.* 225, 397–410. doi:10.1016/j.epsl.2004.07.002

Huang, Y. P., Jiang, Z. L., Li, J. R., Wang, B. Q., and Man, L. (2013). Analysis of tectonic stress direction of Tarim basin during neotectonic period. *Petroleum Geol. Recovery Effic.* 20 (3), 5–9. (in Chinese with English abstract). doi:10.3969/j.issn.1009-9603.2013.03.002

Izquierdo-Llavall, E., Roca, E., Xie, H. W., Pla, O., Munoz, J. A., Rowan, M. G., et al. (2018). Influence of overlapping décollements, syntectonic sedimentation, and structural inheritance in the evolution of a contractional system: The central Kuqa fold-and-thrust belt (tian Shan mountains, NW China). *Tectonics* 37, 2608–2632. doi:10.1029/2017TC004928

Jia, C. Z., Zhang, S. B., and Wu, S. Z. (2004). *Stratigraphy of the Tarim Basin and adjacent areas*. Beijing: Science Press, 1–1063. (upper and lower volumes) [M]. (in Chinese with English abstract).

Jia, C. Z. (2009). The structures of Basin and range system around the Tibetan plateau and the distribution of oil and gas in the Tarim Basin [J]. *Geotect. Metallogenia* 33 (01), 1–9. (in Chinese with English abstract). doi:10.3969/j.issn.1001-1552.2009.01.001

Jolivet, M., Dominguez, S., Charreau, J., Chen, Y., Li, Y. A., and Wang, Q. C. (2010). Mesozoic and Cenozoic tectonic history of the central Chinese Tian Shan: Reactivated tectonic structures and active deformation. *Tectonics* 29, TC6019.

Jolivet, M., Heilbronn, G., Robin, C., Barrier, L., Bourquin, S., Guo, Z. J., et al. (2013). Reconstructing the late palaeozoic – mesozoic topographic evolution of the Chinese tian Shan: Available data and remaining uncertainties. *Adv. Geosciences* 37, 7–18. doi:10.5194/adgeo-37-7-2013

Laborde, A., Barrier, L., Simoes, M., Li, H., Coudroy, T., Van der Woerd, J., et al. (2019). Cenozoic deformation of the Tarim Basin and surrounding ranges (xinjiang, China): A regional overview. *Earth-science Rev.* 197, 102891. doi:10.1016/j.earscirev.2019.102891

Li, B. L., Jia, C. Z., Pang, L. Q., Guan, S. W., Yang, G., Shi, X., et al. (2007). The spatial distribution of the foreland thrust tectonic deformation in the circum-Tibetan plateau Basin and range system [J]. *Acta Geol. Sin.* (09), 1200–1207. (in Chinese with English abstract). doi:10.3321/j.issn:0001-5717.2007.09.005

Li, C., Wang, S. L., and Wang, L. S. (2019). Tectonostratigraphic history of the southern Tian Shan, Western China, from seismic reflection profiling. *J. Asian Earth Sci.* 172, 101–114. doi:10.1016/j.jseaes.2018.08.017

Li, J. F., Zhao, Y., Pei, J. L., Liu, F., Zhou, Z. Z., Gao, H. L., et al. (2017). Cenozoic marine sedimentation problem of the Tarim Basin [J]. *J. Geomechanics* 23 (01), 141–149. (in Chinese with English abstract). doi:10.3969/j.issn.1006-6616.2017.01.010

Li, Q., Li, L., Zhang, Y. Y., and Guo, Z. J. (2020). Oligocene incursion of the paratethys seawater to the Junggar Basin, NW China: Insight from multiple isotopic analysis of carbonate. *Sci. Rep.* 10 (1), 6601. doi:10.1038/s41598-020-63609-0

Li, X., Zhong, D. K., Li, Y., Lei, G. L., Yang, X. Z., Wu, Q. K., et al. (2013). Sedimentary characteristics and evolution of the Neogene and quaternary in Kuqa depression of Tarim Basin [J]. *J. Palaeogeogr.* 15 (02), 169–180. (in Chinese with English abstract). doi:10.7605/gdlxb.2013.02.016

Li, Y. P., Robinson, A. C., Gadoev, M., and Oimuhammadzoda, I. (2020). Was the Pamir salient built along a Late Paleozoic embayment on the southern Asian margin? *Earth Planet. Sci. Lett.* 550, 116554. doi:10.1016/j.epsl.2020.116554

Lin, X., Cheng, X. R., Feng, Y. F., and Peng, B. F. (2019). A review on regressive time in southwest Tarim Basin and its forming mechanism. *Mar. Geol. Quat. Geol.* 39 (03), 84–93. (in Chinese with English abstract). doi:10.16562/j.cnki.0256-1492.2018060301

Liu, C. Y., Zhao, H. G., Zhang, C., and Wang, J. Q. (2009). The important turning period of evolution in the Tibet-Himalaya tectonic domain. *Earth Sci. Front.* 16 (04), 1–12. (in Chinese with English abstract). doi:10.3321/j.issn:1005-2321.2009.04.001

Lou, Q. Q., Xiao, A. C., Zhong, N. C., and Wu, L. (2016). A method of prototype restoration of large depressions with terrestrial sediments: A case study from the cenozoic Qaidam Basin. *Acta Petrol. Sin.* 32 (03), 892–902. (in Chinese with English abstract).

Ma, C. M., Li, J. H., Cao, Z. L., Liu, L. X., and Wang, M. N. (2020). Lithofacies paleogeographic reconstruction and evolution of the Carboniferous-Permian basin group in Central Asia. *Acta Petrol. Sin.* 36 (11), 3510–3522. (in Chinese with English abstract). doi:10.18654/1000-0569/2020.11.16

Ma, T., Ma, Q., Wang, Z. Y., Yuan, C., Hu, J. F., and Wang, H. (2020). Sequence stratigraphic framework and sedimentary evoIution of PaIeogene prototype sedimentary basin in Kuqa Depression. *Chin. J. Geol.* 55 (02), 369–381. (in Chinese with English abstract). doi:10.12017/dzkx.2020.024

Ning, F., Yun, J. B., Li, J. J., Song, H. M., and Zhao, L. D. (2021). Structural characteristics and exploration prospects of the southwestern margin of Bachu Uplift, Tarim Basin [J]. *Oil Gas Geol.* 42 (02), 299–308. doi:10.11743/ogg20210204

Pirouz, M., Simpson, G., and Chiaradia, M. (2015). Constraint on foreland basin migration in the Zagros mountain belt using Sr isotope stratigraphy. *Basin Res.* 27, 714–728. doi:10.1111/bre.12097

Scotese, C. R. (2004). A continental drift flipbook. *J. Geol.* 112 (06), 729–741. doi:10.1086/424867

Shao, L. Y., He, Z. P., Gu, J. Y., Liu, W. L., Jia, J. H., Liu, Y. F., et al. (2006). Lithofacies palaeogeography of the Paleogene in Tarim Basin [J]. *J. Palaeogeogr.* 03, 353–364. (in Chinese with English abstract). doi:10.3969/j.issn.1671-1505.2006.03.008

Song, B. W., Zhang, K. X., Xu, Y. D., Ji, J. L., Luo, M. S., Han, F., et al. (2022). Neogene Tectonic-stratigraphic realms and sedimentary sequence in China. *Earth Sci.* 47 (04), 1143–1161. (in Chinese with English abstract). doi:10.3799/dqkx.2021.072

Sun, J. M., and Jiang, M. S. (2013). Eocene seawater retreat from the southwest Tarim Basin and implications for early Cenozoic tectonic evolution in the Pamir Plateau. *Tectonophysics* 588, 27–38. doi:10.1016/j.tecto.2012.11.031

Sun, J. M., Morteza, S., Nahid, A., Cao, M. M., Zhang, Z. L., Tian, S. C., et al. (2021). Permanent closure of the Tethyan Seaway in the northwestern Iranian Plateau driven by cyclic sea-level fluctuations in the late Middle Miocene. *Palaeogeogr. Palaeoclimatol. Palaeoecol.* 564, 110172. doi:10.1016/j.palaeo.2020.110172

Sun, J. M., Windley, B. F., Zhang, Z. L., Fu, B. H., and Li, S. H. (2016a). Diachronous seawater retreat from the southwestern margin of the Tarim Basin in the late Eocene. *J. Asian Earth Sci.* 116, 222–231. doi:10.1016/j.jseaes.2015.11.020

Sun, J. M., Xiao, W. J., Windley, B. F., Ji, W. Q., Fu, B. H., Wang, J. G., et al. (2016b). Provenance change of sediment input in the northeastern foreland of Pamir related to collision of the Indian Plate with the Kohistan-Ladakh arc at around 47 Ma. *Tectonics* 35 (2), 315–338. doi:10.1002/2015TC003974

Tang, X. D., Tuo, X. S., Mi, D. J., and Qin, H. F. (2014). Research on pronvenance and sedimentrary environment of Suweiyi formation of Bashentamu area, Southwest Tian Shan mountainous region, Xinjiang [J]. *Contributions Geol. Mineral Resour. Res.* 29 (04), 579–586. (in Chinese with English abstract). doi:10.6053/j.issn.1001-1412.2014.04.016

Tapponnier, P., Mattauer, M., Proust, F., and Cassaigneau, C. (1981). Mesozoic ophiolites, sutures, and arge-scale tectonic movements in Afghanistan. *Earth Planet. Sci. Lett.* 52 (2), 355–371. doi:10.1016/0012-821X(81)90189-8

Tapponnier, P., and Molnar, P. (1977). Active faulting and tectonics in China. *J. Geophisical Res.* 82, 2905–2930. doi:10.1029/JB082i020p02905

Todrani, A., Speranza, F., D'Agostino, N., and Zhang, B. (2022). Post-50 Ma evolution of India-Asia collision zone from paleomagnetic and GPS data: Greater India indentation to eastward Tibet flow. *Geophys. Res. Lett.* 49, e2021GL09662.

Wang, B. Q., Wang, Q. H., Han, L. J., Han, J., and Wang, L. G. (2007). Segmentation characteristics and dynamic mechanism of the che'erchen fault in the southeast Tarim basin. *Oil Gas Geol.* (06), 755–761. (in Chinese with English abstract). doi:10.3321/j.issn:0253-9985.2007.06.008

Wang, P., Liu, D. L., Li, H. B., Chevalier, M. L., Wang, Y. D., Pan, J. W., et al. (2021). Sedimentary provenance changes constrain the Eocene initial uplift of the central Pamir, NW Tibetan plateau. *Front. Earth Sci.* 9, 741194. doi:10.3389/feart.2021.741194

Wang, S. H., Zheng, J. Z., Gao, S. Q., Wang, Y. K., Zhang, M. J., Zhou, T. W., et al. (2019). "The play characteristic and exploration potential in sedimentary basins in central Asia," in *Proceedings of the international field exploration and development conference* (Singapore: Springer Singapore), 3487–3494. doi:10.1007/978-981-15-2485-1_321

Wang, T. F., Jin, Z. K., Shi, Z. W., Dai, X. C., and Cheng, R. H. (2020). Phanerozoic plate history and structural evolution of the Tarim Basin, northwestern China. *Int. Geol. Rev.* 62 (12), 1555–1569. doi:10.1080/00206814.2019.1661038

Wang, X., Sun, D. H., Chen, F. H., Wang, F., Li, B. F., Popov, S. V., et al. (2014). Cenozoic paleo-environmental evolution of the Pamir–Tien Shan convergence zone. *J. Asian earth Sci.* 80, 84–100. doi:10.1016/j.jseaes.2013.10.027

Wei, G. Q., Jia, C. Z., Shi, Y. S., Lu, H. F., and Wang, L. S. (2000). Tectonic characteristics and petroleum prospects of cenozoic compound rejuvenated foreland basins in Tarim. *Acta Geol. Sin.* (02), 123–133. (in Chinese with English abstract). doi:10.3321/j.issn:0001-5717.2000.02.004

Wu, G. H., Deng, W., Huang, S. Y., Zheng, D. M., and Pan, W. Q. (2020). Tectonic-paleographic evolution in the Tarim Basin. *Chin. J. Geol.* 55 (02), 305–321. (in Chinese with English abstract). doi:10.12017/dzkx.2020.020

Xia, L. Q., Ma, Z. P., Li, X. M., Xia, Z. C., and Xu, X. Y. (2009). Paleocene-early Eocene (65-40Ma) volcanic rocks in Tibetan plateau: The products of syn-collisional volcanism. *Northwest. Geol.* 42 (03), 1–25. (in Chinese with English abstract). doi:10.3969/j.issn.1009-6248.2009.03.001

Yue, Y., Xu, Q. Q., Fu, H., and Xi, D. P. (2017). Reservior-cap rock assemblage and sedimentary characteristics of Cretaceous-Paleogene in southwest Tarim Basin. *Petroleum Geol. Exp.* 39 (03), 318–326. (in Chinese with English abstract). doi:10.11781/sysydz201703318

Zhang, G. Y., Tong, X. G., Xin, R. C., Wen, Z. X., Ma, F., Huang, T. F., et al. (2019). Evolution of lithofacies and paleogeography and hydrocarbon distribution worldwide (II). *Petroleum Explor. Dev.* 46 (5), 896–918. doi:10.1016/S1876-3804(19)60248-X

Zhang, H., Liu, C. L., Cao, Y. T., Sun, H. W., and Wang, L. C. (2013). A tentative discussion on the time and the way of marine regression from Tarim bay during the cenozoic. *Acta Geosci. Sin.* 34 (05), 577–584. (in Chinese with English abstract). doi:10.3975/cagsb.2013.05.08

Zhang, J. Y., Xing, F. C., Krijgsman, W., Zhang, C., Wei, W., Chen, L., et al. (2022). Palaeogeographic reconstructions of the eocene-oligocene Tarim Basin (NW China): Sedimentary response to late Eocene sea retreat. *Palaeogeogr. Palaeoclimatol. Palaeoecol.* 587, 110796. doi:10.1016/j.palaeo.2021.110796

Zhang, S. J., Hu, X. M., Han, Z., Li, J., and Garzanti, E. (2018). Climatic and tectonic controls on Cretaceous-Palaeogene sea-level changes recorded in the Tarim epicontinental sea. *Palaeogeogr. Palaeoclimatol. Palaeoecol.* 501, 92–110. doi:10.1016/j.palaeo.2018.04.008

Zhang, Y., Zheng, M. L., Chen, J. J., Deng, M. Z., Tian, F. L., Zhang, W. K., et al. (2021). Geometrical and kinematical characteristics of the mazartag fault zone in Bachu uplift, Tarim Basin. *Oil Gas Geol.* 42 (02), 325–337. (in Chinese with English abstract). doi:10.11743/ogg20210206

Zhang, Y., Zwingmann, H., Liu, K., and Luo, X. (2011). Hydrocarbon charge history of the Silurian bituminous sandstone reservoirs in the Tazhong uplift, Tarim Basin, China. *AAPG Bull.* 95 (3), 395–412. doi:10.1306/08241009208

Zhao, H. F., Wei, Y. Y., Shen, Y., Xiao, A. C., Mao, L. G., Wang, L. Q., et al. (2016). Cenozoic tilting history of the south slope of the Altyn Tagh as revealed by seismic profiling: Implications for the kinematics of the Altyn Tagh fault bounding the northern margin of the Tibetan Plateau. *Geosphere* 12, 884–899. doi:10.1130/GES01269.1

Zheng, M. L., Wang, Y., Jin, Z. J., Li, J. C., Zhang, Z. P., Jiang, H. S., et al. (2014). Superimposition, evolution and petroleum accumulation of Tarim Basin. *Oil Gas Geol.* 35 (06), 925–934. (in Chinese with English abstract). doi:10.11743/ogg20140619

Zhuang, X. J., Xiao, L. X., and Yang, J. (2002). Sedimentary facies in southwestern region of Tarim Basin. *Xinjiang Geol.*, 78–82. (in Chinese with English abstract). doi:10.3969/j.issn.1000-8845.2002.z1.014